Communication

Single-Crystalline CeB Nanowires

Han Zhang, Qi Zhang, Jie Tang, and Lu-Chang Qin

J. Am. Chem. Soc., **2005**, 127 (22), 8002-8003• DOI: 10.1021/ja051340t • Publication Date (Web): 12 May 2005

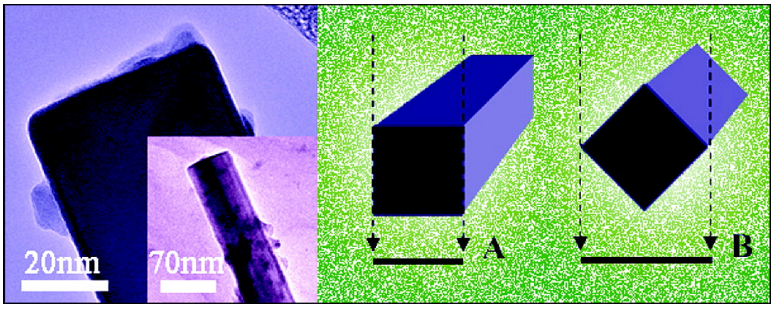

J|A|C|S
COMMUNICATIONS

Published on Web 05/12/2005

Single-Crystalline CeB_6 Nanowires

Han Zhang,[†] Qi Zhang,[‡] Jie Tang,[‡,§] and Lu-Chang Qin*[,†,‡]

Curriculum in Applied and Materials Sciences and Department of Physics and Astronomy, University of North Carolina at Chapel Hill Chapel Hill, North Carolina 27599-3255, and National Institute for Materials Science, Tsukuba, Japan

Received March 3, 2005; E-mail: lcqin@physics.unc.edu

Single-crystalline rare-earth hexaborides, especially lanthanum hexaboride (LaB_6) and cerium hexaboride (CeB_6), are thermionic cathode materials widely used in a broad range of electron beam applications where a high brightness electron source with long service life is required. The advantage of using rare-earth hexaboride originated from its crystal structure, which is composed of rare-earth metal atoms embedded inside a stable boron octahedron network.[1] This arrangement allows a unique combination of all the desired properties for an excellent cathode material, such as low work function, low volatility, low electrical resistivity, high mechanical strength, and high chemical resistance, while these properties seldom coexist in any other materials. Compared to LaB_6, CeB_6 is believed to have even lower work function (~2.5 eV) and lower volatility, which mean lower operation temperature and longer service life when used as a thermionic electron emitter.[2,3] The low work function is even more crucial a criterion when a cathode material is designed for field-induced electron emission applications, which offer a brightness 100 or more times higher than a thermionic electron source. Field emission current density J can be expressed by the Fowler−Nordheim equation:[4]

$$J = 1.5 \times 10^{-6}(E^2/\phi)\exp(10.4/\phi^{1/2} - 6.44 \times 10^7\phi^{3/2}/E)\mathrm{A/cm}^2$$

where E is the local electric field produced at the tip and ϕ is the work function of the emitting surface of the tip. It can be inferred that the emission current density J is enhanced almost exponentially with the decrease of work function ϕ. However, to achieve a high emission current density J, high local electric field E is another important factor and can be expressed as $E = V/5r$, with V being the voltage applied on the emitter tip and r being the tip radius. The difficulty in making single-crystalline rare-earth hexaboride sharp tips has impeded the development of field emission cathode from this low work function material. Several attempts were made to fabricate electrolytically sharpened LaB_6 and CeB_6 needle-shaped field emitters from bulk single crystals, but no satisfactory field emission results have been reported, in contrast to the highly expected low turn-on voltage and high emission current promised by the low work function that these hexaborides possess.[5−9] On the other hand, sharper tips and higher aspect ratio will also enhance field emission for a given material. In a recent communication, we reported a successful synthesis of ⟨111⟩ oriented LaB_6 nanowires with diameter below 100 nm.[10] In a subsequent article, we reported the fabrication of ⟨001⟩ oriented LaB_6 nanowires and measurement of their field emission characteristics where a field emission current density of about 5×10^5 A/cm^2 was obtained at a driving voltage of 800 V.[11] In this communication, we present the successful synthesis of single-crystalline CeB_6 nanowires with lateral dimension around 50 nm, length more than several micrometers, and a well-defined ⟨001⟩ crystal growth direction.

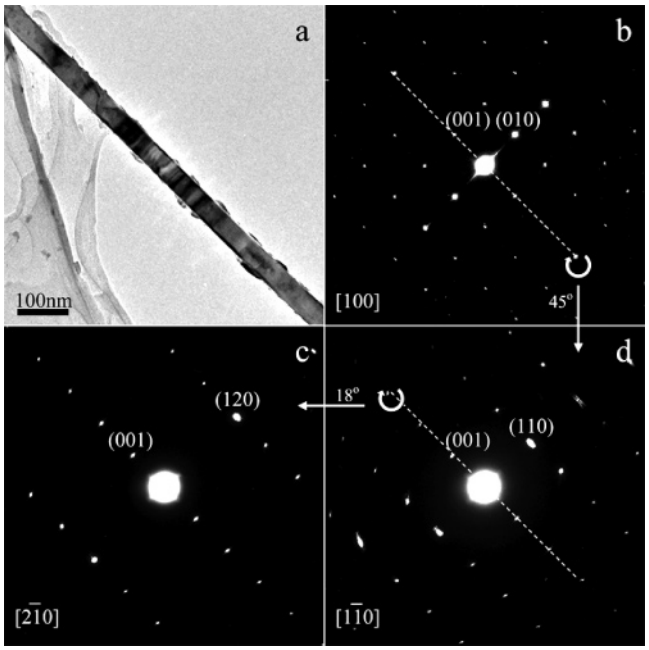

Figure 1. (a) Low-magnification TEM image of a CeB_6 nanowire. (b−d) Electron diffraction patterns of the same CeB_6 nanowire tilted to zone axes [100], [1$\bar{1}$0], and [2$\bar{1}$0], respectively. Dashed lines indicate the tilting axes about which the nanowire is rotated to the desired orientation. Circular arrows indicate the tilting angles, and the straight arrows point to the tilting sequence in experiment.

The synthesis is based on the following chemical reaction:

$$2CeCl_3(g) + 12BCl_3(g) + 21H_2(g) = 2CeB_6(s) + 42HCl(g)$$

The reaction was conducted in a tube furnace operated at 1125 °C where the BCl_3 gas (Aldrich, 99.9%) was introduced to the reaction zone in a quartz tube and $CeCl_3$ powders (Aldrich, 99.9%) were vaporized in a quartz boat placed inside the same tube furnace. A silicon substrate coated with platinum was placed at a position downstream of the quartz boat for CeB_6 nanowire deposition.

After the reaction, CeB_6 nanowires with lateral dimensions ranging from below 50 nm to more than 1 μm were grown on the substrate surface. The nanowires were examined in both scanning electron microscope (SEM, JEM-6300) equipped with an energy-dispersive X-ray spectrometer (EDX, KevexSigma3) and transmission electron microscope (JEM-2010F operated at 200 kV). EDX analysis indicates that these nanowires are composed of B and Ce elements.

A representative morphological study and structure determination of the nanowires are presented in Figure 1. Figure 1a is a typical

[†] Curriculum in Applied and Materials Sciences, University of North Carolina.
[‡] Department of Physics and Astronomy, University of North Carolina.
[§] National Institute for Materials Science.

10.1021/ja051340t CCC: $30.25

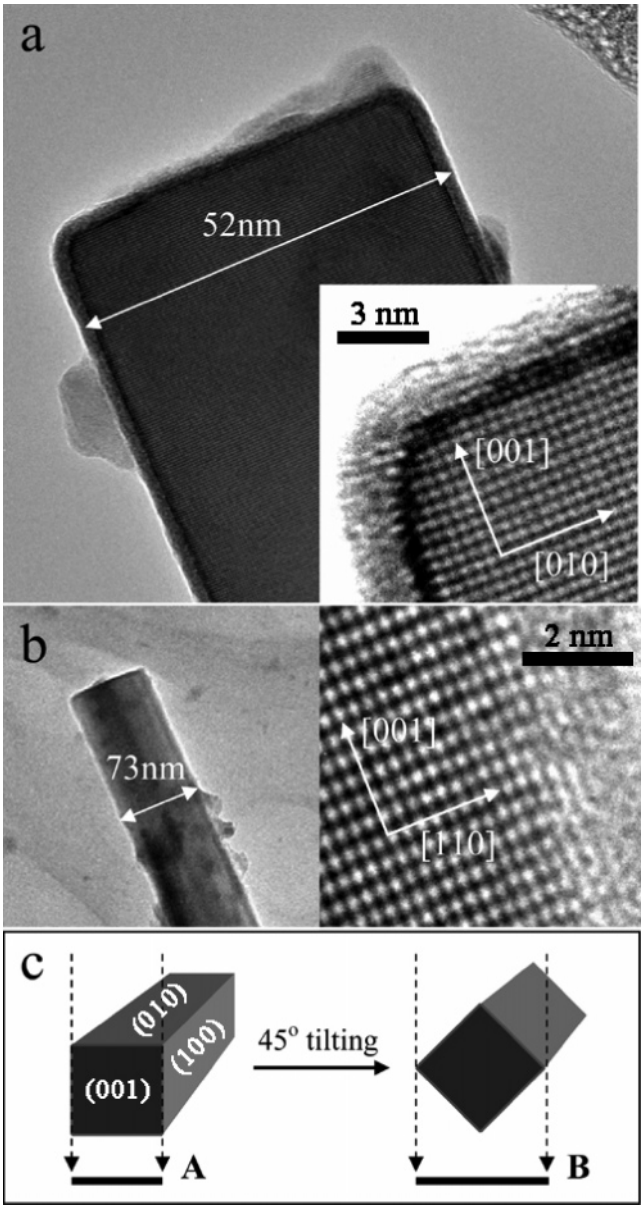

Figure 2. (a) [100] direction TEM image of the CeB_6 nanowire tip. Inset is a high-resolution lattice image of the tip's top left corner. (b) [1$\bar{1}$0] direction TEM image of the same nanowire together with a high-resolution lattice image showing its right-side wall. (c) Illustration of the 45° tilting process to reconstruct the morphology of the nanowire.

TEM image at low magnification showing a straight nanowire with smooth surfaces of lateral dimension around 50 nm and length extending more than 10 μm. Parts b−d of Figure 1 show three electron diffraction patterns taken along three different crystal zone axes of the same nanowire to identify the CeB_6 crystal lattice, which has a primitive cubic structure of space group *Pm*3*m* and has lattice constant $a = 0.4129$ nm. The three zone axes are [100] (Figure 1b), [2$\bar{1}$0] (Figure 1c), and [1$\bar{1}$0] (Figure 1d). The relative orientational relationship between the three electron diffraction patterns are also given in the figures. For example, the [1$\bar{1}$0] zone axis electron diffraction pattern (Figure 1d) was obtained by tilting the nanowire 45° about its [001] direction (illustrated in Figure 1b).

Due to the important role of the emitter tip in the emission properties, a morphological study of the tip area of a typical CeB_6 nanowire was also conducted as shown in Figure 2. Figure 2a is a TEM image showing that the CeB_6 nanowire has a flat tip top, and its lateral dimension is measured to be 52 nm in this orientation. A high-resolution electron microscopy (HRTEM) image of the top left corner the CeB_6 nanowire is displayed in the inset. We found that, similar to the LaB_6 nanowires,[11] the growth direction is the [001] axis of the crystal and both the flat tip top and the nanowire side surfaces are terminated with the {100} lattice planes. Figure 2b is a TEM image of the same tip after a 45° tilting about the axial direction of the nanowire. As expected, the electron diffraction pattern confirmed that the nanowire was oriented in the [1$\bar{1}$0] zone axis, as also shown in the HRTEM image in Figure 2b. Moreover, since now the projected width of the nanowire at this angle is 73 nm, which makes a ratio of $\sqrt{2}$ with that obtained in Figure 2a, it suggests that the nanowire has a square cross section. This morphology of the nanowire is also indicated in the left image of Figure 2b, where a darker contrast line appears in the middle of the nanowire due to the largest thickness in the diagonal direction of the nanowire of a square cross section. A schematic summary of the nanowire morphology is illustrated in Figure 2c: both the tip of the nanowire and the side surfaces are terminated with the {100} crystallographic lattice planes as labeled in the illustration; the dashed arrows represent the direction in which the electron beam is incident with the projections labeled underneath using letters A and B, which correspond to the images given in Figure 2a and Figure 2b, respectively. After checking several other nanowires among the same sample, we obtained similar results except that some nanowires have cross sections that are rectangular rather than square. The fact that catalyst particles were sometimes seen at the end of the nanowires suggests that the formation of the CeB_6 nanowires is likely a vapor−liquid−solid process.

In conclusion, we have developed a chemical vapor deposition method that is able to produce successfully CeB_6 nanowires of well-defined morphology. The nanowires have a square cross section with width of about 50 nm and have lengths extending more than 10 μm. The growth direction of the nanowires is the ⟨001⟩ lattice direction, and they have flat tips and walls that are all terminated by the {100} lattice planes. These CeB_6 nanowires are of potential use as point electron emitters for applications including providing thermionic emission, field-induced emission, and thermal field-induced emission of electrons for TEM, SEM, flat panel displays, as well as other electronic devices that require high-performance electron sources.

Acknowledgment. We wish to thank the UNC Research Council for financial support and J.T. is also partially supported by Japan-U.S. Collaborative Scientific Research Program of JSPS.

References

(1) Lafferty, J. M. *J. Appl. Phys.* **1951**, *22*, 299.
(2) Swanson, L. W.; McNeely, D. R. *Surf. Sci.* **1979**, *83*, 11.
(3) Davis, P. R.; Gesley, M. A.; Schwind, G. A.; Swanson, L. W. *Appl. Surf. Sci.* **1989**, *37*, 381.
(4) Brodie, I.; Spindt, C. A. In *Advances in Electronics and Electron Physics*; Hawkes, P. W., Ed.; Academic Press: San Diego, CA, 1992; Vol. 83, Ch. 2.
(5) Shimizu, R.; Kataoka, Y.; Tanaka, T.; Kawai, S. *Jpn. J. Appl. Phys.* **1975**, *14*, 1089.
(6) Futamoto, M.; Hosoki, S.; Okano, H.; Kawabe, U. *J. Appl. Phys.* **1977**, *48*, 3541.
(7) Nagata, H.; Harada, K.; Shimizu, R. *J. Appl. Phys.* **1990**, *68*, 3614.
(8) Harada, K.; Nagata, H.; Shimizu, R. *J. Electron Microsc.* **1991**, *40*, 1.
(9) Okano, H.; Futamoto, M.; Hosoki, S.; Kawabe, U. *Shinkai* **1977**, *20*, 127.
(10) Zhang, H.; Zhang, Q.; Tang, J.; Qin, L.-C. *J. Am. Chem. Soc.* **2005**, *127*, 2862.
(11) Zhang, H.; Zhang, Q.; Zhao, G., Yang, G.; Zhang, J.; Tang, J.; Zhou, O.; Qin, L.-C. In press.

JA051340T